Cell Stem Cell
Article

Tet1 and Tet2 Regulate 5-Hydroxymethylcytosine Production and Cell Lineage Specification in Mouse Embryonic Stem Cells

Kian Peng Koh,[1] Akiko Yabuuchi,[2] Sridhar Rao,[2] Yun Huang,[1,10] Kerrianne Cunniff,[2] Julie Nardone,[3] Asta Laiho,[4] Mamta Tahiliani,[1] Cesar A. Sommer,[5] Gustavo Mostoslavsky,[5] Riitta Lahesmaa,[1,4] Stuart H. Orkin,[2,6,7] Scott J. Rodig,[8] George Q. Daley,[2,6,7,9] and Anjana Rao[1,10,*]

[1]Immune Disease Institute and Program in Cellular and Molecular Medicine, Children's Hospital Boston, Boston, MA 02115, USA
[2]Division of Pediatric Hematology/Oncology, Children's Hospital Boston and Dana-Faber Cancer Institute, Harvard Stem Cell Institute, Boston, MA 02115, USA
[3]Bioinformatics, Cell Signaling Technology, Danvers, MA 01923, USA
[4]Turku Centre for Biotechnology and The Finnish Microarray and Sequencing Centre, University of Turku and Åbo Akademi University, FI-20520 Turku, Finland
[5]Section of Gastroenterology, Department of Medicine, and Center for Regenerative Medicine, Boston University School of Medicine, Boston, MA 02118, USA
[6]Howard Hughes Medical Institute, Boston, MA 02115, USA
[7]Harvard Stem Cell Institute, Cambridge, MA 02138, USA
[8]Department of Pathology, Brigham and Women's Hospital, Boston, MA 02115, USA
[9]Department of Biological Chemistry and Molecular Pharmacology, Harvard Medical School, Boston, MA 02115, USA
[10]Present address: La Jolla Institute for Allergy and Immunology, La Jolla, CA 92037, USA
*Correspondence: arao@idi.harvard.edu or arao@liai.org
DOI 10.1016/j.stem.2011.01.008

SUMMARY

TET family enzymes convert 5-methylcytosine (5mC) to 5-hydroxymethylcytosine (5hmC) in DNA. Here, we show that *Tet1* and *Tet2* are Oct4-regulated enzymes that together sustain 5hmC in mouse embryonic stem cells (ESCs) and are induced concomitantly with 5hmC during reprogramming of fibroblasts to induced pluripotent stem cells. ESCs depleted of *Tet1* by RNAi show diminished expression of the Nodal antagonist *Lefty1* and display hyperactive Nodal signaling and skewed differentiation into the endoderm-mesoderm lineage in embryoid bodies in vitro. In Fgf4- and heparin-supplemented culture conditions, *Tet1*-depleted ESCs activate the trophoblast stem cell lineage determinant *Elf5* and can colonize the placenta in midgestation embryo chimeras. Consistent with these findings, *Tet1*-depleted ESCs form aggressive hemorrhagic teratomas with increased endoderm, reduced neuroectoderm, and ectopic appearance of trophoblastic giant cells. Thus, 5hmC is an epigenetic modification associated with the pluripotent state, and Tet1 functions to regulate the lineage differentiation potential of ESCs.

INTRODUCTION

The methylation status of DNA influences many biological processes during mammalian development and is known to be highly aberrant in cancer (Gal-Yam et al., 2008; Ooi et al., 2009). DNA methylation is a powerful mechanism of genome defense against transposons and other parasitic DNA (Goll and Bestor, 2005); in addition, promoter methylation in mammals has long been considered suppressive for gene expression (Klose and Bird, 2006). Recent whole-genome analyses have provided insights into the complexity of methylation patterns in plant and animal species (Farthing et al., 2008; Feng et al., 2010a; Lister et al., 2009; Meissner et al., 2008; Zemach et al., 2010). DNA methylation occurs primarily at CpG dinucleotides in mammals: CpG methylation marks that are lost on newly replicated DNA strands are faithfully restored by the maintenance DNA methyltransferase Dnmt1. In embryonic stem cells (ESCs), however, a substantial fraction of cytosine methylation occurs in non-CpG contexts, where it has been attributed to the activity of the de novo methyltransferases Dnmt3a and Dnmt3b (Lister et al., 2009; Ramsahoye et al., 2000).

Dynamic changes in DNA methylation occur during early embryogenesis (reviewed in Feng et al., 2010b). Shortly after fertilization, the paternal genome loses the methylcytosine mark prior to DNA replication, whereas the maternal genome loses the mark passively in early cell cycles before blastulation. De novo methylation by Dnmt3 occurs around the time of blastocyst implantation, to a greater extent in the inner cell mass (ICM), which remains pluripotent and gives rise to all cell types of the embryo proper, than in the outer trophectoderm (TE) layer, which is restricted to an extraembryonic fate and gives rise to the placenta (Reik et al., 2001). During the formation of primordial germ cells in the mouse, a second wave of genome-wide demethylation occurs during which imprinted marks are erased; they are subsequently reset in the developing gametes through de novo DNA methylation. The tight regulation of DNA methylation and demethylation is developmentally of crucial importance

because Dnmt-deficient (and therefore hypomethylated) ESCs and embryos lose lineage restriction and show transdifferentiation to the extraembryonic trophoblast lineage (Jackson et al., 2004; Ng et al., 2008).

We recently identified the TET proteins TET1, TET2, and TET3 as a new family of enzymes that alter the methylation status of DNA (Iyer et al., 2009; Tahiliani et al., 2009). TET proteins are 2-oxoglutarate (2OG)- and Fe(II)-dependent dioxygenases that catalyze the hydroxylation of 5-methylcytosine to 5-hydroxymethylcytosine (5hmC) in DNA. TET proteins and 5hmC have been reported in many different tissues, and both 5hmC and Tet expression/activity are tightly regulated during ESC differentiation (Ito et al., 2010; Ko et al., 2010; Kriaucionis and Heintz, 2009; Szwagierczak et al., 2010; Tahiliani et al., 2009). TET1 and TET2 are both implicated in cancer: TET1 is an MLL partner in rare cases of acute myeloid (AML) and lymphoid (ALL) leukemias, and loss-of-function of TET2 is strongly associated with AML as well as a variety of myelodysplastic syndromes and myeloproliferative disorders (see references in Ko et al., 2010). Together, these data suggest that dysregulation of DNA methylation via TET proteins and hmC may have a role in ESC pluripotency, oncogenic transformation (especially of hematopoietic stem cells toward the myeloid lineage), and neuronal function.

Here, we describe the function of Tet proteins (and, by inference, 5hmC) in mouse ESCs. ESC lines are culture explants from the inner cell mass (ICM) of the developing blastocyst. They can be maintained in the proliferative, undifferentiated state in culture by using the cytokine leukemia inhibitory factor (LIF) to activate STAT3 and the serum component bone morphogenetic protein (BMP) to induce inhibitor-of-differentiation proteins. When given the appropriate cellular signals, they can differentiate into cellular derivatives of the three primary germ layers: ectoderm, mesoderm, and endoderm. Withdrawal of LIF from serum-containing media allows BMP to switch from supporting self-renewal to inducing mesodermal and endodermal differentiation while blocking entry into neural lineages; when grown in the absence of both LIF signals and serum, ESCs are predisposed to convert to a neuronal fate (Ying et al., 2003a, 2003b). These features of self-renewal and ability to differentiate, characteristic of a pluripotent state, require a high degree of epigenetic plasticity. Genes crucial for pluripotency are kept active by a self-organizing network of transcription factors and are rapidly silenced by histone modifications and DNA methylation during differentiation, whereas genes that are required later in cellular differentiation are held in a transiently repressed state by chromatin modifications that are easily reversed. Because Tet proteins modify DNA methylation status, it was conceivable that they might influence the expression and functions of either or both classes of genes.

RESULTS

Tet1 and Tet2 Regulate 5hmC Levels in Mouse ESCs and Are Associated with the Pluripotent State

In culture conditions containing LIF and serum, *Tet1* transcripts are present at high copy numbers in mouse ESCs, comparable to those of the pluripotency factor *Oct4*; *Tet2* transcripts are about 5-fold less abundant than *Tet1* but still well expressed; and *Tet3* transcript levels are very low (Figure 1A). Individual depletion of *Tet1* or *Tet2* mRNAs with SMARTpool siRNA duplexes (Figure S1A available online) resulted in a moderate decrease in 5hmC, whereas combined depletion of both enzymes reduced 5hmC levels by 75%–80% (Figures 1B and 1C; Figures S1B and S1C). Thus, Tet1 and Tet2 together are responsible for the bulk of 5hmC production in mouse ESCs cultured in the presence of LIF. In contrast to a previous report (Ito et al., 2010), we did not observe major changes in ESC morphology upon siRNA-mediated depletion of either *Tet1* alone or both *Tet1* and *Tet2* (Figure S1D).

When plated on gelatin in the presence of LIF, ESCs largely retained expression of *Tet1*, *Tet2*, and *Oct4* over 4 to 5 days. Within 3 days of LIF withdrawal, *Tet1* and *Tet2* mRNA levels declined to 25%–30% of starting levels, with a time course that paralleled the decline of *Oct4* mRNA (Figure 1D), and differentiated epithelial-like cells were observed in 4 to 5 days. When the ESCs were treated with retinoic acid (RA; a potent stimulus for cellular differentiation) at the same time that LIF was withdrawn, *Tet1*, and *Oct4* expression declined more rapidly (Figure 1D), and epithelial-like morphology was apparent earlier, by day 3. *Tet3* mRNA levels increased more than 10-fold under these conditions (Figure 1D). Under both conditions, 5hmC levels declined significantly, to 40%–60% of control (Tahiliani et al., 2009; Figure 1E); the moderate change (compared to that seen in Figures 1B and 1C) likely reflects both the incomplete loss of *Tet1* and *Tet2* under conditions of LIF withdrawal and the upregulation of *Tet3* in response to RA (Figure 1D).

We examined *Tet* expression and activity during reprogramming of mouse embryonic fibroblasts (MEFs) into induced pluripotent stem cells (iPSCs) by transduction with the four reprogramming transcription factors Oct4, Sox2, Klf4, and c-Myc (Takahashi and Yamanaka, 2006). The starting population of fibroblasts expressed almost no *Tet1* mRNA and only a basal level of *Tet2* mRNA, but fully reprogrammed iPSCs that had reactivated an endogenous Oct4-GFP reporter (Yeom et al., 1996) displayed levels of *Tet1* and *Tet2* mRNA comparable to those in ESCs; *Tet3* transcripts also decreased, approaching the low level observed in ESCs (Figure 1F). In parallel, 5hmC levels increased, both globally and at MspI sites, from almost undetectable in fibroblasts to levels typical of ESCs in iPSCs (Figure 1G). Similar results were obtained during reprogramming of mouse adult tail-tip fibroblasts into iPSCs (data not shown). Collectively, these data point to a strong association of Tet1, Tet2, and 5hmC with the pluripotent state in both ESCs and iPSCs and a contrasting association of Tet3 with the differentiated state.

Oct4 Regulates *Tet* mRNA Levels

We measured *Tet* mRNA levels during ESC differentiation induced by RNAi-mediated depletion of the key pluripotency factors *Oct4*, *Sox2*, and *Nanog*. ESCs treated with SMARTpool siRNA duplexes targeting *Oct4* differentiated rapidly within 3 days. Differentiation induced by *Sox2* RNAi was slower, requiring ~5 days, but alkaline phosphatase-positive colonies were still present in ESCs treated with *Nanog* RNAi for 5 days (Figure S2A). We confirmed that each SMARTpool depleted expression of its target pluripotency factor (Figure S2B), although as expected, depletion of each pluripotency factor in

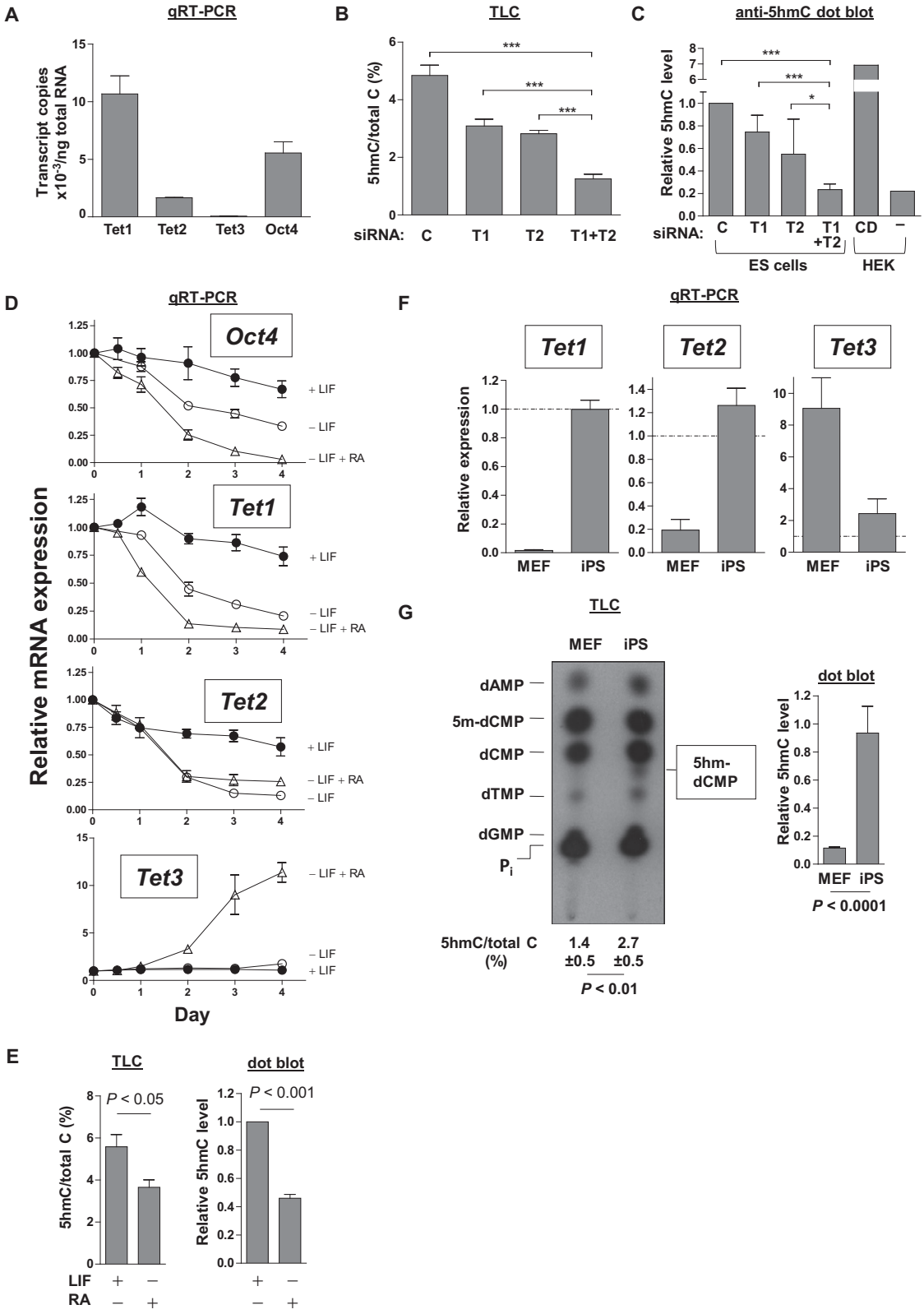

Figure 1. Tet1 and Tet2 Regulate 5hmC Levels in Mouse ESCs and Are Associated with the Pluripotent State

(A) Normalized transcript copy numbers of *Tet1*, *Tet2*, *Tet3*, and *Oct4* in v6.5 mouse ESCs, determined using absolute standard curves of plasmid templates. *Gapdh* transcript levels were used to estimate RNA content.

ESCs also downregulated expression of the others because of known cross-regulatory and cooperative interactions (Chew et al., 2005; Loh et al., 2006).

Oct4 and *Sox2* RNAi resulted in potent repression of *Tet1* and *Tet2* mRNA, to < 20% and ~30% of control levels, respectively; *Tet3* mRNA was upregulated by ~4-fold and ~2-fold (Figure 2A). *Nanog* RNAi had almost no effect on *Tet1* and *Tet3* while reducing *Tet2* expression moderately, to ~60% of control. TLC analysis at day 5 showed a marked loss of 5hmC at MspI sites only in cells treated with *Oct4* siRNA (Figure 2B).

Chromatin immunoprecipitation of biotin-tagged Oct4 from ESCs stably expressing the BirA biotin ligase (Kim et al., 2008) showed that Oct4 bound to sites located within conserved noncoding sequence (CNS) regions of both the *Tet1* and *Tet2* genes (Figures 2C–2H). In both cases, the sites resembled consensus Oct4-Sox2 composite sites (Loh et al., 2006) and especially the *Oct4* portion of the site was strongly conserved between human and mouse (Figures 2E and 2H). Oct4 binding sites were not detected in other CNS regions of the *Tet1* locus (Figures S2C and S2D) or at two other predicted Oct4-Sox2 binding elements in CNS regions at ~−140 kb and −200 kb 5′ of the *Tet2* transcription start site. Although we have not tested formally whether these conserved Oct4-Sox2 composite sites function as transcriptional regulatory elements, the combined data suggest strongly that *Tet1* and *Tet2* are regulated by the Oct4-Sox2 complex.

Tet1 Depletion Skews ESC Differentiation

We characterized gene expression in ES cells after siRNA-mediated depletion of each of the three *Tet* proteins by quantitative RT-PCR. *Tet* mRNAs were maximally depleted by 3 days of transfection. *Tet1* depletion had no effect on *Tet2* mRNA expression and vice versa (Figure S1A). In contrast to a previous report that *Tet1* depletion led to diminished *Nanog* mRNA and protein (Ito et al., 2010), *Tet* depletion did not affect expression of the key pluripotency factors *Oct4*, *Sox2* and *Nanog* under our conditions for up to 5 days (Figure 3A), nor was there a marked change in the undifferentiated appearance of ESCs maintained in LIF (Figure S1D). Rather, *Tet1* depletion resulted in reproducible changes in expression of a panel of lineage-specific markers within 3–5 days: there was a reproducible increase in expression of mRNAs encoding the trophectoderm markers *Cdx2*, *Eomes*, and *Hand1*, and a consistent decrease in expression of the neuroectoderm markers *Pax6* and *Neurod1* and the Nodal antagonists *Lefty1* and *Lefty2* (Figure 3A, Figure S3A, and data not shown). *Tet2* depletion had no effect on trophectoderm, endoderm, and mesoderm markers but consistently caused a small increase in expression of *Pax6*, *Neurod1*, *Lefty1*, and *Lefty2* (Figure 3A and Figure S3A), whereas *Tet3* knockdown caused a 50% repression of *Lefty2* but otherwise had no effect on all other targets tested (Figure S3A and data not shown). Combined depletion of *Tet1* and *Tet2*, shown above to decrease genomic 5hmC levels almost to baseline (Figures 1B and 1C), had a similar but less striking effect compared to *Tet1* depletion alone (Figure 3A), suggesting that Tet2 antagonizes the dominant effect of Tet1 at specific target genes.

To explore the effect of prolonged depletion of *Tet1* on ESC developmental potential, we generated ESC clones stably expressing shRNAs against *Tet1* and *Tet2*. Two *Tet1*-depleted clones, generated using *Tet1* shRNA#2, showed >80% decrease in *Tet1* mRNA levels (Tet1-kd/shRNA#2.1 and #2.2; Figure S3B, left); likewise, two *Tet2*-depleted clones, generated using *Tet2* siRNA sequences #1 and #3, showed ~55% and ~75% decrease in *Tet2* mRNA levels, respectively (Tet2-kd/shRNA#1 and #3; Figure S3B, right). Control clones expressed an irrelevant shRNA (scramble [Scr]-kd) or shRNA directed against *GFP* (GFP-kd). The clones could be propagated serially on feeder cells in the absence of further selection and were morphologically indistinguishable from parental and control clones (Figure S3C). Growth proliferation rates of the selected Tet-kd clones were similar to or slightly enhanced compared to control clones (Figure S3D). Whole-genome transcriptome analysis of stable Tet1-kd versus control ESC clones largely confirmed the results from transient RNAi transfections; gene ontology (GO) analysis of differentially expressed genes yielded many terms related to embryonic development and cell-cycle regulation (Table S1). Possibly because of incomplete knockdown, most gene-expression changes in Tet1-kd ESCs were fairly modest (~2- to 5-fold), and the cells retained a genome-wide molecular signature typical of normal ESCs.

We injected control shRNA and Tet-kd ES clones intramuscularly into immunodeficient mice and observed teratoma

(B) Densitometric measurement of 5′-hydroxymethyl-dCMP (5hm-dCMP) spot intensities detected on thin layer chromatography (TLC) analysis of enriched CpG sites in the genome of ESCs after 5 days of siRNA transfection to deplete *Tet1* and/or *Tet2*. Values are depicted as percentages of total dCMP species comprising 5-methyl-dCMP (5m-dCMP), dCMP, and hm-dCMP. Error bars indicate SD of seven replicates from three independent experiments. siRNA treatments are denoted: C, control; T1, Tet1 SMARTpool; T2, Tet1 SMARTpool; T1+T2, combined Tet1+Tet2 SMARTpool. A representative TLC autoradiogram is shown in Figure S1B. For ESC morphology and knockdown efficiency of *Tet1* and *Tet2*, see Figure S1.

(C) Measurement of 5hmC levels in genomic DNA from transfected ESCs and HEK293T based on antibody dot blot. Values are expressed relative to levels in control-transfected ESCs. HEK293T cells were transfected with either TET1-catalytic domain (CD) or mock-transfected (−). Error bars indicate SD of five replicates from two experiments. In (B) and (C), p values derived from ANOVA with Bonferroni's multiple comparison test are denoted: *$p < 0.05$; ***$p < 0.001$.

(D) Quantitative RT-PCR measurement of *Oct4*, *Tet1*, *Tet2*, and *Tet3* transcript levels in mouse ESCs cultured for 1–4 days on gelatinized (feeder-free) plates in the presence of LIF, or differentiated by LIF withdrawal, or LIF withdrawal plus addition of 1 μM all-*trans* retinoic acid (RA). Data are represented as mean ± SEM from three independent experiments.

(E) Measurement of hmC levels by TLC (left) and dot blot (right) in genomic DNA extracted from ESCs after 4 days of LIF withdrawal and treatment with RA. Error bars indicate SD of 3–5 replicates.

(F) Quantitative RT-PCR of *Tet1*, *Tet2*, and *Tet3* transcript levels expressed relative to levels in ESCs (marked as dotted lines), during reprogramming of MEFs by viral transduction of *Oct4*, *Sox2*, *Klf4*, and *c-Myc* into iPSC clones. Error bars indicate SD (n = 3).

(G)TLC (left) and hmC dot blot (right) analyses showing 5hmC detected in iPSCs, but not in fibroblasts. hmC levels from dot blots are expressed relative to levels in ESCs. Error bars indicate SD of 3-5 replicates. p values in (E) and (G) are derived from t tests.

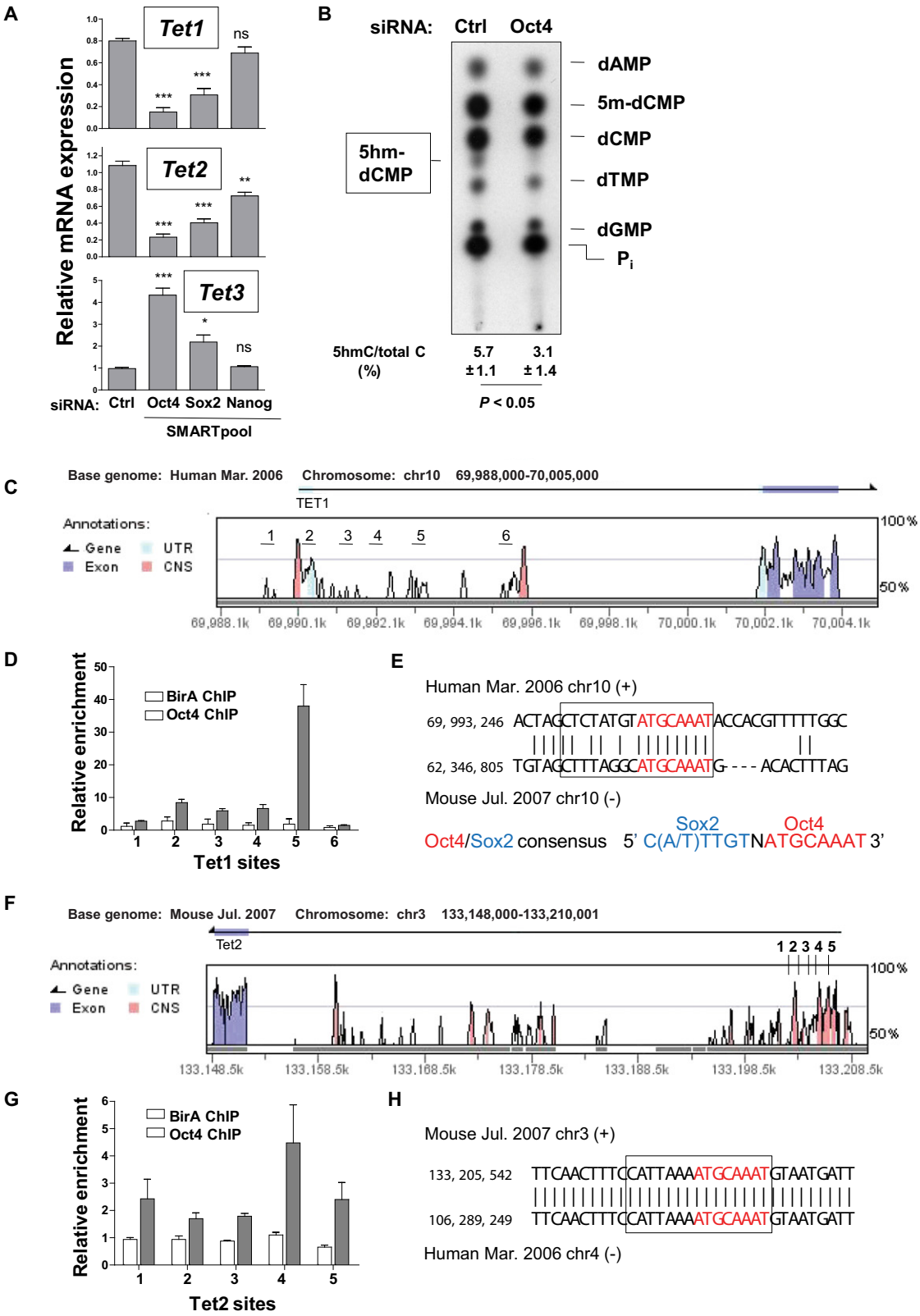

Figure 2. *Tet* mRNA Levels Are Regulated by Oct4

(A) Quantitative RT-PCR of *Tet1*, *Tet2*, and *Tet3* transcript levels in ESCs transfected for 5 days with *Oct4*, *Sox2*, and *Nanog* SMARTpool siRNA. Normalized transcript levels are expressed relative to levels at the start of transfection. Data are mean ± SEM from three experiments. p values derived from ANOVA with

formation. Within 4–7 weeks, control ESC lines formed well-differentiated benign teratomas containing cells representative of all three embryonic germ layers, whereas Tet1-kd clones formed large aggressive tumors with massive internal hemorrhage (Figures 3B–3D). Histologically, all three primary germ layer lineages could be found in Tet1-kd teratomas, but the relative contributions of each lineage appeared altered compared to controls (Figures 3C-D). Tet1-kd teratomas contained predominantly immature glandular tissue with surrounding stromal cells, indicative of definitive endoderm and mesoderm respectively; many of the glandular cells contained nuclei in mitotic phases, suggestive of a highly proliferative state (Figure 3E). There was considerably less neuroectoderm in the teratoma and many regions with necrotic tissue and blood (Figure 3D). A striking feature was the presence of many giant cells with large nuclei, found especially within and near the necrotic regions but also forming distinct clusters (Figure 3F); many of these cells contained glycogen-rich inclusion bodies, indicative of trophoblastic giant cells of the extra-embryonic lineage (Figure 3G). These histological features were independent of tumor size because sized-matched control teratomas grown to full size were typically not hemorrhagic, contained more neural tissue, and rarely contained any trophoblastic giant cells. Moreover, smaller Tet1-kd teratomas obtained with injection of fewer cells (10^5 instead of 10^6) still formed hemorrhagic tumors containing many giant cells (Figures S3E and S3F).

Like Tet1-kd clones, Tet2-kd clones also formed large hemorrhagic teratomas that grew more aggressively than controls (Figure 3H). Both Tet2-kd clones, generated by stable expression of independent shRNA hairpins, displayed a similar phenotype of hemorrhagy, although the phenotype was stronger in Tet2-kd/shRNA#3-derived teratomas, correlating with stronger constitutive *Tet2* knockdown (Figure S3A, right). Despite the hemorrhagic appearance, there was more neuroectoderm contribution in Tet2-kd teratomas, such that apart from the appearance of regions with necrotic tissue, most cellular features still resembled those of control teratomas (Figure 3I). Trophoblastic giant cells were also less apparent in Tet2-kd compared to Tet1-kd teratomas, appearing in clusters in only one oversized tumor harvested but otherwise barely represented in all other Tet2-kd tumors (data not shown). We conclude that *Tet1* loss-of-function in ESCs results in developmental skewing toward endoderm/mesoderm and trophoblast lineages, whereas *Tet2* loss-of-function maintains a tendency toward neuroectoderm.

Altered Developmental Potential of *Tet1*-Depleted ESCs: Skewing to Trophectoderm

The upregulation of transcripts encoding the trophectodermal transcription factors *Cdx2* and *Eomes* (Figure 3A), and the appearance of trophoblastic giant cells in Tet1-kd tumors (Figures 3F–3IG), suggested that *Tet1* deficiency might attenuate the normal restriction of ESCs to embryonic tissues and permit their transdifferentiation into extra-embryonic trophoblast derivatives. Indeed, a previous report showed that when *Tet1* siRNA was injected together with a marker gene into mouse embryos at the two-cell stage, the marked (presumably *Tet1*-depleted) cells were moderately excluded from the inner cell mass (ICM) and enriched in the trophectoderm (Ito et al., 2010).

To explore this phenotype further, we cultured control and Tet1-kd clones on feeders in the presence of FGF4 and heparin, but without exogenous LIF, a culture condition previously described to favor the derivation of trophoblast stem (TS) cells from the trophectoderm of blastocysts (Tanaka et al., 1998). In these alternative "TS" culture conditions, *Tet1* depletion did not result in obvious morphological changes: both control (scramble shRNA) and Tet1-kd ESCs formed dense undifferentiated colonies that tended to be flatter with jagged edges, thus showing some resemblance to true TS cells, which are flat with a ridge-like periphery (Figure S4A). After 2 weeks in TS cell culture conditions, we observed a robust and reproducible induction of *Elf5* transcripts in Tet1-kd clones (50- to 200-fold increase in *Elf5* mRNA over the low background expression seen in control clones, approaching ~10%–20% of the levels observed in TS cells; Figure 4A). *Elf5* lies downstream of the early trophoblast lineage determinants *Cdx2* and *Eomes* and was recently described as a commitment marker for the trophoblastic fate (Ng et al., 2008). Moreover, whole-genome gene set enrichment analysis of Tet1-kd clones compared to control clones in TS conditions revealed significant enrichment (both FDR q value and FWER p value of 0.02) of a core set of genes defining trophectodermal cell differentiation, including *Cdx2*, *Eomes*, and *Tead4* (Figure S4B). Expression of intermediate trophoblast (*Tpbpa*) or differentiated giant cell markers (*PL1*) in Tet1-kd clones was not observed during the course of TS cell culture, suggesting that the cells were being sustained in a TS-like state without overt differentiation into trophoblasts. To further investigate trophectoderm skewing, we cultured the Tet1-kd/shRNA#2.1 ESC clone for 2 weeks in TS culture conditions, picked three subclones, Tet1-kd/shRNA#2.1-sc1, .2,

Bonferroni's multiple comparison test are denoted: *p < 0.05; **p < 0.01; ***p < 0.001. For ESC morphology and knockdown efficiency of *Oct4*, *Sox2*, and *Nanog*, see Figure S2.

(B) TLC analysis of genomic DNA purified from mouse ESCs differentiated by *Oct4* RNAi. Values of 5hmC levels are mean ± SD of three replicates from two independent experiments.

(C) Vista plot of sequence conservation between the human and mouse *Tet1* gene loci upstream of the first coding exon, depicting CNS regions in the vicinity of the *Tet1* transcription start site and coding exon 1. Regions numbered 1 to 6 spaced at 1 kb intervals were probed by ChIP PCR. For a diagram of all the CNS regions in the *Tet1* locus, see Figure S2C.

(D) Oct4 binding was detected as amplification from Oct4 biotin-mediated ChIP samples from ESCs at the target sites depicted in (C). Control ChIP was performed in cells expressing only the biotin ligase (BirA). For a complete analysis of Oct4 binding to all CNS regions in the *Tet1* locus, see Figure S2D.

(E) The mouse-human sequence alignment at the *Tet1* site 5 showing a conserved *Oct4-Sox2* consensus element (boxed). The Oct4 consensus sequence is highlighted in red.

(F) Sequence conservation between the human and mouse *Tet2* gene loci upstream of the first coding exon. Regions numbered 1 to 5 spaced at 1 kb intervals were probed.

(G) Oct4 binding was detected as amplification from Oct4 biotin-mediated ChIP samples from ESCs at the target sites depicted in (F).

(H) The mouse-human sequence alignment at the *Tet2* site 4 showing a conserved *Oct4-Sox2* consensus element (boxed).

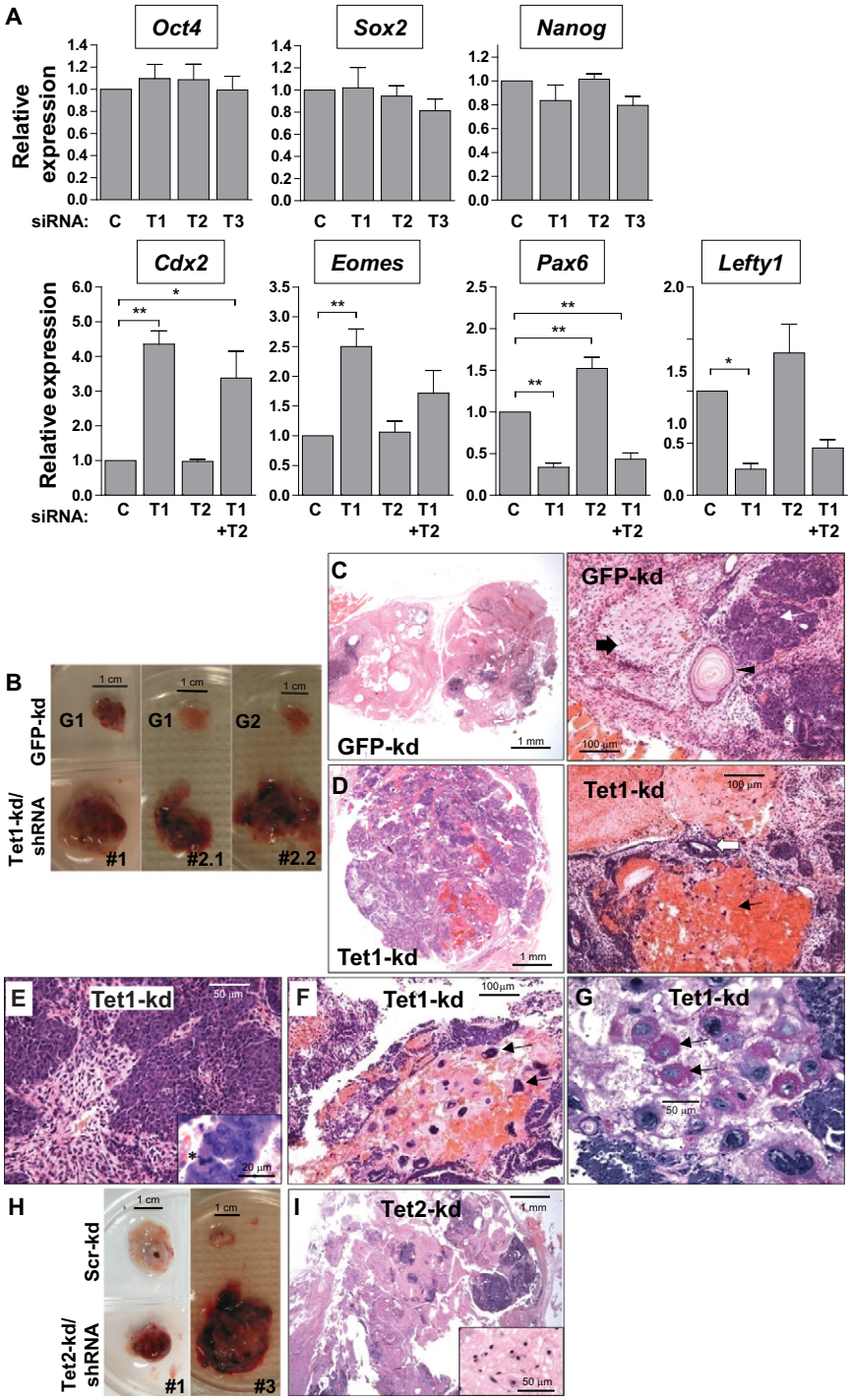

Figure 3. *Tet* Depletion Selectively Affects Cell Lineage Markers and Skews ESC Differentiation

(A) Effect of Tet1 (T1), Tet2 (T2), Tet3 (T3), or combined Tet1+Tet2 (T1+T2) SMARTpool siRNAs on the expression of pluripotency and selected lineage marker genes, assessed after 5 days of transfection. C, non-targeting control siRNA. Data are represented as mean ± SEM, n = 3 to 4. *p < 0.05; **p < 0.01; ***p < 0.001 by ANOVA with a post-hoc test for comparison to control. See also Figure S3A.

(B) Enhanced growth and extensive hemorrhagy in Tet1-kd tumors compared to GFP-kd controls. Refer to Figure S3 for knockdown efficiency in stable Tet-kd ESC clones.

(C) Gross histology of teratomas formed after injection of control clones, revealed through low-power images of hematoxylin/eosin (H&E)-stained sections (left), showing high contribution of differentiated neuronal tissue (pink). A higher power image (right) shows mature epithelium with squamous differentiation (arrowhead), terminally differentiated neuronal tissue (block arrow), and immature glandular tissue (white arrow).

(D) Low-power image of a Tet1-kd teratoma (from Tet1-kd/shRNA#2.1), showing predominance of immature glandular tissue (purple). A higher power image (right) shows necrotic tissue with blood and scattered giant cells (black arrow) and glandular tissue (white arrow).

(E) Tet1-kd teratoma showing highly proliferative glandular tissues. Inset: a cell undergoing mitosis is marked with asterisk.

(F) Tet1-kd teratoma showing a cluster of trophoblastic giant cells (arrows).

(G) Periodic acid-Schiff staining of a serial section from the Tet1-kd tumor shown in (F), showing glycogen-rich granules (purple stain) in giant cells (arrows).

(H) Hemorrhagy in Tet2-kd tumors compared to scrambled-kd controls.

(I) Low-power image of H&E-stained Tet2-kd teratoma (from Tet2-kd/shRNA#3), showing areas of fully differentiated neuronal tissue (pink) and glandular tissue (purple). Inset, neuronal tissue.

Histology of Tet1-kd shown is representative of tumors from Tet1-kd/shRNA#2 (each clone #2.1 and #2.2 injected into two mice per experiment) from three independent experiments performed with two different strains of immunodeficient mice. Each Tet2-kd clone was injected in two mice per experiment in two independent experiments.

and .3 based on flattened TS-like morphology, and propagated them in TS culture conditions. Quantitative RT-PCR analysis of these subclones showed a dramatic induction of *Cdx2*, *Eomes*, and *Elf5* expression compared to control shRNA and parental cell lines (Figure 4B); again, however, expression of these TE markers in the subclones was only a fraction of levels in TS cells, suggesting that the cells are propagating as an intermediate cell type between the ESC and TS cell states.

The association of *Tet1* knockdown with *Cdx2*, *Eomes*, and *Elf5* activation suggested that Tet1 might function to repress trophectoderm development during early embryogenesis. To test this hypothesis, we injected GFP-labeled Tet1-kd ESC lines, cultured either in ESC or TS cell conditions, into mouse blastocysts and observed chimerism in mid-gestation (E10.5) embryos by GFP fluorescence. Typically, ESCs injected into the ICM of blastocysts contribute only to the developing embryo and not

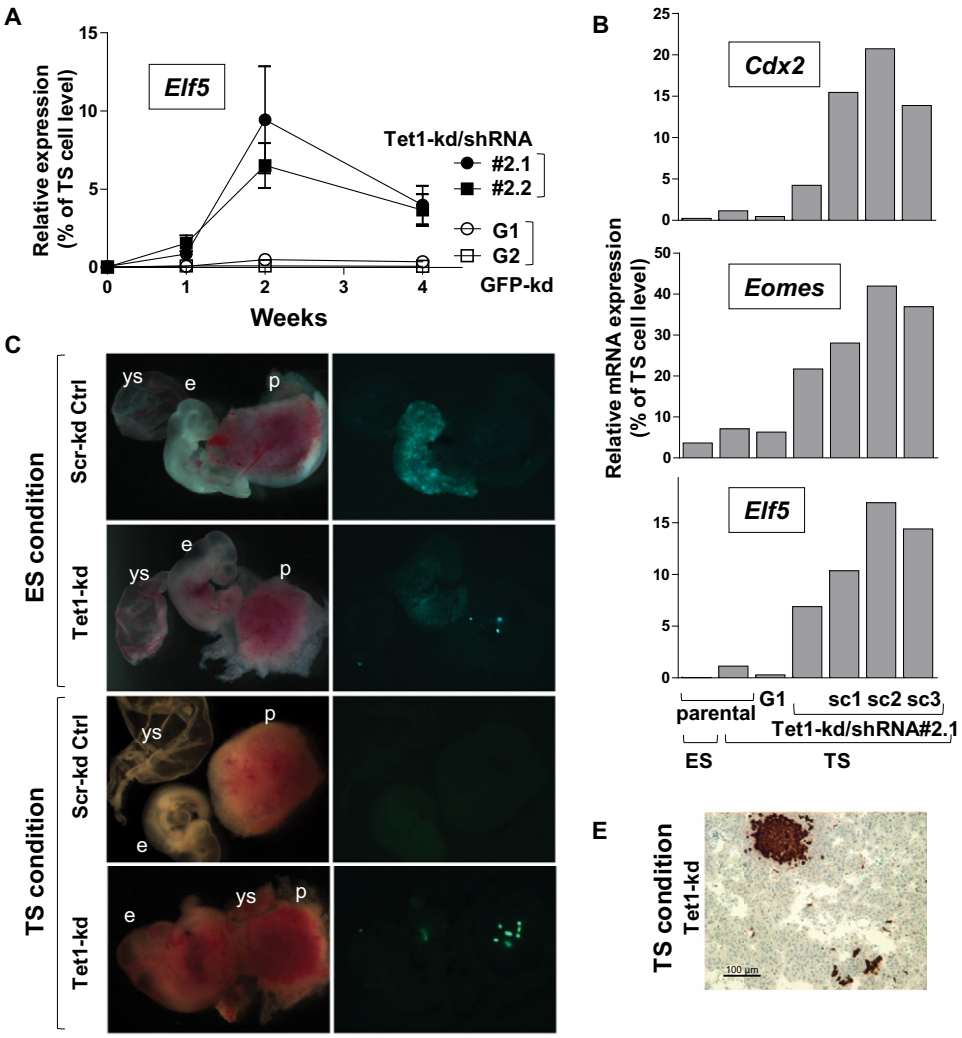

D

		No. of embryos (transfers)	No. of GFP+ embryos (%)	No. of GFP+ placentas (%)
ES	control	16 (4)	13 (81.3%)	0 (0%)
	Tet1-kd	35 (5)	17 (48.6%)	1 (2.9%)
TS	control	26 (4)	1 (3.8%)	0 (0%)
	Tet1-kd	59 (8)	7 (11.9%)	3 (5.1%)

Figure 4. *Tet1* Depletion in ESCs Predisposes Cells to Differentiate along a Trophoblastic Lineage

(A) Time-course of expression of *Elf5* in control and Tet1-kd clones grown in TS conditions for 1–4 weeks. Data represent mean ± SEM of four independent experiments.

(B) Expression of trophectoderm markers *Cdx2*, *Eomes*, and *Elf5* in the Tet1-kd/shRNA#2 line and subclones cultured in TS cell conditions for 4 weeks compared to parental cells in TS cell or ESC conditions. Normalized transcript levels in (B) and (C) are expressed relative to levels in TS cells (set as 100).

(C) Midgestation embryo chimerism of GFP-labeled control (scrambled shRNA) or Tet1-knockdown (Tet1-kd/shRNA#2) cells injected into blastocysts after culture in ES or TS conditions. Brightfield (left) and whole-mount GFP fluorescence (right) images were taken at E10.5. e, embryo; ys, yolk sac; p, placenta.

(D) Scoring of GFP presence in embryos and placentas at midgestation.

(E) GFP antibody staining of placental section showing chimerism of a Tet1-kd subclone (sc3) from TS cell culture.

to placental tissues (Beddington and Robertson, 1989), and this was indeed observed with ESCs expressing a scrambled control shRNA (Figure 4C). Tet1-kd ESCs from ESC cultures also chimerized the developing embryo, consistent with our data from teratomas that differentiation into the three primary germ layers is not completely blocked; however, the contribution to embryos appeared reduced and in rare cases, GFP$^+$ cells could even be detected in placental tissue (manifested as spots of

extraembryonic GFP$^+$ cells in one embryo, or as faint GFP$^+$ cells in another 2/35 embryos obtained from five uterine transfers) (Figure 4D). When the same GFP-labeled ESCs were cultured for 4 weeks in TS cell conditions, there was a marked reduction in the ability of both control and Tet1-kd clones to chimerize the embryos based on GFP fluorescence; this, in part, reflects a technical shortcoming because of silencing of GFP observed in prolonged TS culture conditions. However, injection of a Tet1-kd clone or subclone from TS cell culture occasionally produced embryos with bright aggregates of GFP-positive cells in the placenta (Figure 4C). The presence of GFP$^+$ cells in the placenta was confirmed by immunohistochemical staining for GFP (Figure 4E). In contrast, none of the control ESCs expressing control shRNA gave rise to any bright GFP-fluorescent cells in the placenta, whether cultured under ESCs or TS conditions. Together, these data suggest that a small subset of Tet1-kd ESCs cultured in either ESCs or TS conditions are able to cross an embryonic restriction barrier to colonize the placenta.

Altered Developmental Potential of *Tet1*-Depleted ESCs: Skewing to Mesendoderm

We asked whether the observed increase in the representation of cells of the mesoderm and endoderm lineages in teratomas formed from Tet1-kd ESCs (Figure 3D) could reflect decreased expression of the Nodal antagonist *Lefty* (Figure 3A). Nodal and Lefty are both members of the TGFβ superfamily (Schier, 2009; Shen, 2007; Tabibzadeh and Hemmati-Brivanlou, 2006). Nodal signals act as morphogens and are essential for the induction of mesoderm and definitive endoderm in the gastrulation-stage embryo when uncommitted epiblast cells move through the primitive streak, a structure marked by expression of the transcription factor *Brachyury* (*Bry*) (Tam and Loebel, 2007). Mesoderm is induced from the posterior primitive streak in response to Wnt or low levels of TGFβ/Nodal/Activin signaling, whereas definitive endoderm arises in response to high, sustained Nodal/Activin signals from "mesendoderm" progenitors in the anterior posterior streak that are marked by expression of *Foxa2* and *Goosecoid*. We postulated that *Tet1* depletion, by decreasing *Lefty* expression, would increase Nodal signals and result in the mesoderm/endoderm skewing observed in our teratoma assays.

To test this hypothesis, we used the CD4-Foxa2/GFP-Bry ESC line (E14.1, 129/Ola) in which Brachyury and Foxa2 expression are read out as expression of GFP and a cell-surface receptor, human CD4, respectively (Gadue et al., 2006). If *Tet1* depletion in this cell line indeed led to mesoderm and/or endoderm skewing, this would be apparent in ESC in vitro differentiation assays as increased expression of *Brachyury* and/or *Foxa2*, respectively. We depleted *Tet1* in CD4-Foxa2/GFP-Bry ESCs using two independent *Tet1* siRNAs and then allowed the cells to differentiate into embryoid bodies (EB) for 4 days. During the last 2 days of differentiation, we supplemented some cultures with graded concentrations of TGFβ family member Activin A (1, 5, or 25 ng/ml) as a positive control to stimulate mesoderm and endoderm formation. Unlike Nodal, Activin is not inhibited by Lefty (Chen and Shen, 2004). As expected, *Tet1* transcripts declined to ~50% of control levels by day 2 of EB formation (Figure 1D), but siRNA treatment decreased *Tet1* mRNA expression even further (data not shown). Control siRNA-transfected ESCs remained CD4- and GFP-negative during EB differentiation, but treatment with *Tet1* siRNA (especially siRNA#2) led to the emergence of subpopulations expressing CD4 and GFP indicating strong expression of Foxa2 and low expression of Brachyury, respectively (Figure 5A, top panels; Figure 5B). GFP-Bry and CD4-Foxa2 expression were increased in *Tet1* siRNA-treated cells that were also exposed to low concentrations of activin (5 ng/ml) (Figure 5A, middle panels; Figure 5B). Similarly, when stable Tet1-kd ESC clones (v6.5 cell line) were subjected to in vitro EB differentiation, we again observed induction of *Foxa2* and *Brachyury* as measured by qRT-PCR (Figure 5C).

We examined Nodal/Activin signaling in whole-cell lysates of control and *Tet1*-depleted EB at day 4 by western blotting (Figure 5D). In control-siRNA-treated cells, high doses of Activin A (25 ng/ml) stimulated Smad2 phosphorylation, upregulation of Eomes, and upregulation of Lefty (Figure 5D, lane 4; the Lefty antiserum recognizes both Lefty 1 and Lefty 2; note the particularly strong upregulation of high molecular weight forms of Eomes.) These results are consistent with previous reports that Eomes is a downstream target of Nodal/Activin signaling (Arnold et al., 2008; Brennan et al., 2001) and that both Nodal itself and the inhibitor Lefty are induced by Nodal/Activin signals in positive and negative autoregulatory feedback loops (Besser, 2004; Saijoh et al., 2000). Notably, *Tet1*-depleted ESCs also showed increased Smad2 phosphorylation and increased Eomes expression in the absence of activin (particularly striking in the case of *Tet1* siRNA#2, lane 9), suggesting that decreased levels of *Tet1* promote increased signaling in the TGFβ pathway. These effects of *Tet1* depletion were potentiated by activin treatment (lanes 7, 10, and 11). Interestingly, *Tet1* depletion abolished the activin-induced increase in Lefty expression.

Tet1 Depletion Has Complex Effects on DNA Methylation at Target Gene Promoters

Tet enzymes regulate DNA methylation by modifying 5mC and have been proposed to promote DNA demethylation in multiple ways (Tahiliani et al., 2009). By converting 5mC to 5hmC, Tet proteins diminish DNA methylation. Moreover, because 5hmC is not recognized by Dnmt1, its presence would promote passive demethylation. Finally, 5hmC might be actively removed by a DNA repair system and replaced by unmodified cytosine. Consistent with these possibilities, the *Nanog* promoter has been reported to become hypermethylated in ESCs depleted of *Tet1* (Ito et al., 2010). In contrast, however, we have shown that Tet2 loss-of-function in myeloid tumors results in global hypomethylation rather than localized hypermethylation at CpG dinucleotides in the genome (Ko et al., 2010).

To investigate the relation of *Tet1* depletion to changes in DNA methylation, we examined the promoters of two Tet1-regulated genes, *Lefty1* and *Elf5*. The *Lefty1* promoter is hypomethylated in stem cells and hypermethylated in differentiated cells (Farthing et al., 2008), whereas the *Elf5* promoter is hypermethylated (and repressed) in ESCs compared to TS cells (Ng et al., 2008). We first examined DNA "methylation" at the *Lefty1* promoter in ESCs depleted of *Tet1* by RNAi, using the bisulfite sequencing technique, which does not distinguish 5mC and 5hmC (Huang et al., 2010). Compared to control-treated cells in which the locus was hypomethylated, Tet1-depleted ESCs showed an increase in CpG "methylation" levels at specific regions of the

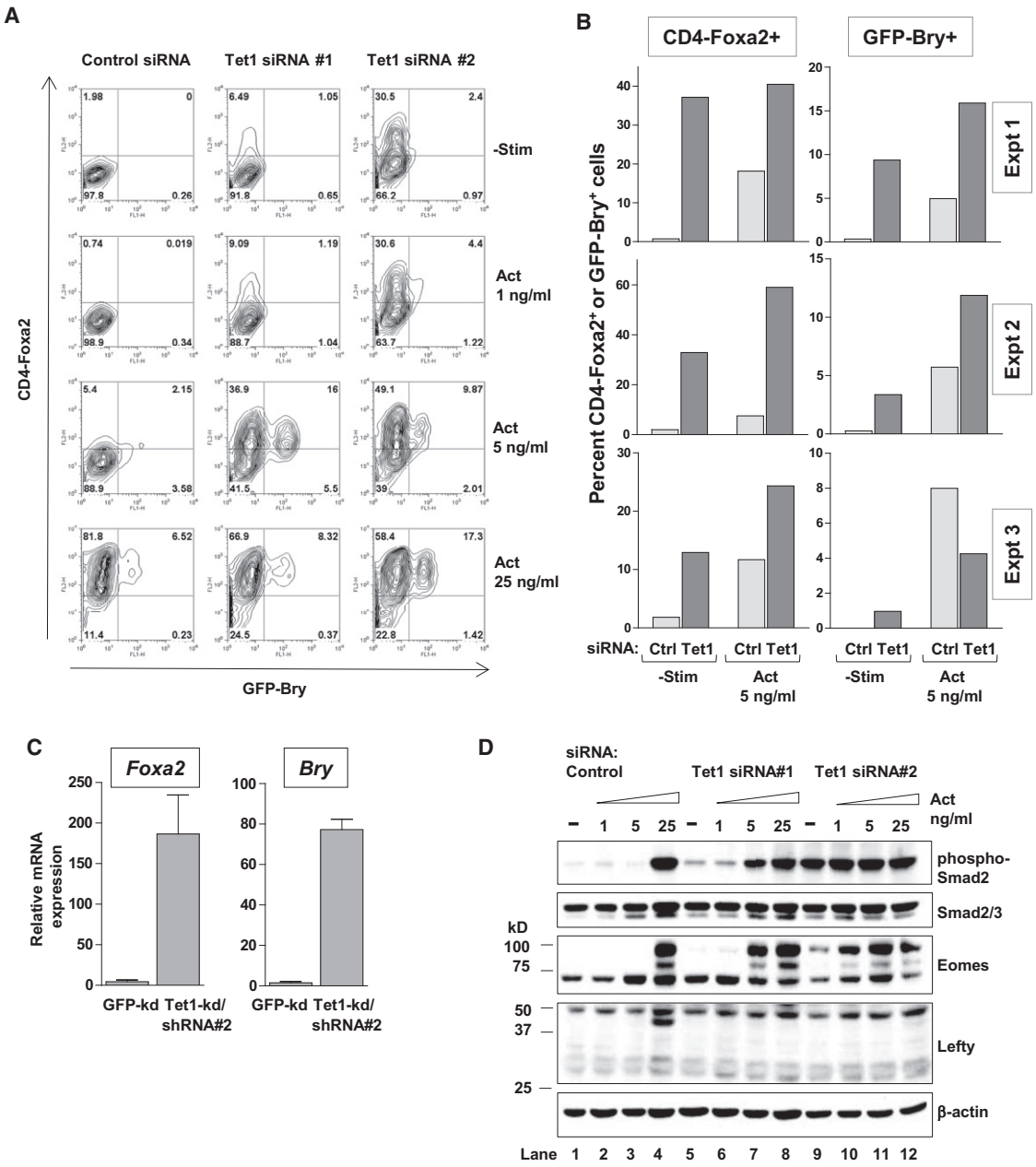

Figure 5. RNAi Depletion of *Tet1* in ESCs Skews Differentiation toward the Endoderm-Mesoderm Lineages In Vitro

(A) Expression of CD4 and GFP in CD4-Foxa2/GFP-Bry ESCs transfected with *Tet1* siRNA and differentiated in serum-free media for 4 days to form EB. EB cultures were reaggregated and treated with Activin A (Act) at the indicated concentrations at day 2. Numbers in quadrants denote percentage of gated cell populations.

(B) Percentages of CD4-high and GFP-high cell populations in Day 4 EB after siRNA treatment. Three independent experiments are shown comparing control and *Tet1* siRNA#2 treatments.

(C) Quantitative RT-PCR analysis of *Foxa2* and *Brachyury* in day 4 EB differentiated from Tet1-kd/shRNA#2 stable clones. Data are mean ± SEM of three clones in each group, representative of two independent experiments.

(D) Western blot analysis of phospho-Smad2, total Smad2/3, Eomes, and Lefty in whole-cell lysates of day 4 EB.

1.4 kb *Lefty1* promoter region (Figure 6A), consistent with the notion that Tet1 directly or indirectly regulates *Lefty1* expression by facilitating DNA demethylation. In contrast, the *Elf5* promoter was as highly ''methylated'' in Tet1-kd ESC subclones as in the parental ESCs (Figure 6B), despite the fact that *Elf5* transcripts were more highly expressed (Figures 4A and 4B).

DISCUSSION

In this study, we report the functional roles of Tet proteins, a newly-discovered family of DNA-modifying enzymes, in mouse ESCs and iPSCs. We show that Tet1 and Tet2 are the key enzymes responsible for the presence of 5hmC in mouse ESCs

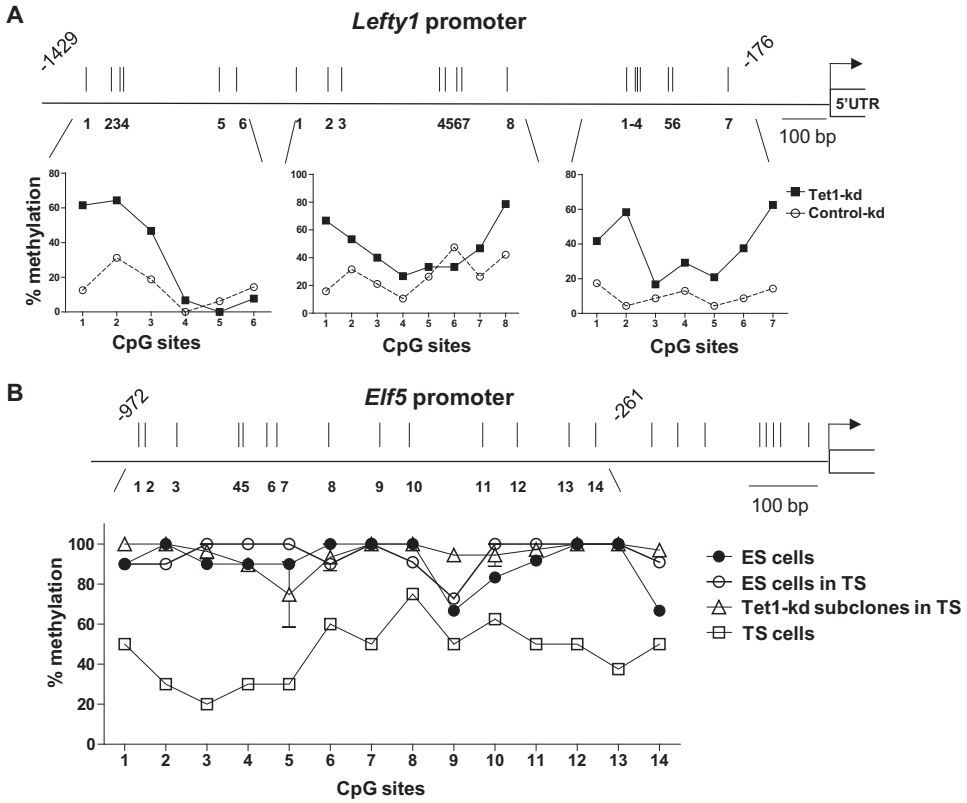

Figure 6. *Tet1* Depletion Has Different Effects on DNA Methylation at Target Gene Promoters

(A) Bisulphite sequencing analysis of CpG methylation status at the *Lefty1* promoter in ESCs transfected with control or *Tet1* SMARTpool siRNA. The average percent methylation at each CpG site is derived from sequencing of 20–24 clones.

(B) Bisulphite sequencing analysis of the *Elf5* promoter in ESCs, TS cells, and various Tet1-kd ES clones in TS culture condition. The percent methylation at each CpG site is derived from sequencing of 10–12 clones. Three Tet1-kd/shRNA#2.1 subclones were analyzed, and errors bars are mean ± SEM.

and iPSCs, that their expression is regulated by Oct4, and that their activity (as judged by 5hmC levels) correlates closely with the pluripotent state. In contrast to a previous report (Ito et al., 2010), acute RNAi-mediated depletion of *Tet1* alone, or both *Tet1* and *Tet2*, did not in our hands cause overt ESC differentiation, diminish ESC proliferation, or affect expression of the key pluripotency factors *Oct4*, *Sox2*, and *Nanog*. Rather, *Tet1* depletion correlated with decreased expression of the Nodal antagonists *Lefty1* and *Lefty 2*, increased expression of the mesoderm/endoderm transcription factors *Brachyury* and *Foxa2*, and increased expression of the trophoectoderm transcription factors *Cdx2*, *Eomes*, and *Elf5*. While we have not yet established whether these genes are direct or indirect targets of Tet1, it is notable that each lies at a "crossroads" of cell-fate determination during embryonic development (Ng et al., 2008; Tabibzadeh and Hemmati-Brivanlou, 2006).

Tet enzymes are downstream targets of the transcription factor network that maintains ESC pluripotency. *Oct4* depletion led to rapid ESC differentiation, a parallel strong decrease in *Tet1* and *Tet2* mRNA expression, and an increase in *Tet3* mRNA expression. *Sox2* RNAi had a similar but less dramatic effect. BIO-ChIP assays showed Oct4 binding to both the *Tet1* and *Tet2* loci at composite Oct4/Sox2 sites, suggesting strongly that *Tet1* and *Tet2* are directly regulated by the cooperative Oct4/Sox2 complex. A previous genome-wide ChIP-seq analysis showed Oct4 binding to the *Tet2* locus (Chen et al., 2008); however, neither this nor earlier studies (Boyer et al., 2005; Kim et al., 2008; Loh et al., 2006) identified *Tet1* or *Tet3* as Oct4 target genes, possibly because the signals did not reach statistical significance. We note that the mild effect of *Nanog* depletion on *Tet2* gene expression may be indirect, through the ability of Nanog to regulate Oct4 and Sox2 (Loh et al., 2006).

Our studies highlight a strong correlation between *Tet1* and *Tet2* expression and the pluripotent state. Stimuli that induced ESC differentiation—LIF withdrawal, RA addition, and *Oct4* RNAi—caused loss of *Tet1* and *Tet2* expression and a parallel loss of genomic 5hmC. A previous kinetic analysis of gene expression in ESCs undergoing RA-induced differentiation also identified *Tet1* (D10Ertd17e) as one of 65 rapidly downregulated candidate genes (Ivanova et al., 2006); however, Tet1 was not characterized further in this study, because—as also observed in our hands—shRNA-mediated knockdown of Tet1 did not dramatically affect morphology or alkaline phosphatase activity in ESCs. Conversely, reprogramming of fibroblasts to iPSCs was associated with increases in *Tet1*, *Tet2*, and 5hmC, and combined depletion of both *Tet1* and *Tet2* during early reprogramming by doxycycline-inducible RNAi reduced the number of iPSC colonies by about 50% (K.P.K., C.A.S., G.M., and A.R., unpublished data). A formal demonstration of the role of Tet enzymes in iPSC reprogramming will require the use of

robust overexpression systems as well as fibroblasts from Tet-deficient mice.

At several genes examined (e.g., *Cdx2*, *Eomes*, *Lefty*, *Pax6*), the effects of *Tet1* depletion were dominant over an often mildly opposing effect of *Tet2* depletion. Since both enzymes catalyze the conversion of 5mC to 5hmC, it is likely that they are recruited to disparate (possibly overlapping) sets of target genes and in turn recruit distinct transcriptional regulatory complexes through their divergent N-terminal regions. Notably, *TET2* and 5hmC are also expressed, albeit at lower levels, in other tissues and cell types including hematopoietic stem cells (HSCs) (Delhommeau et al., 2009; Ito et al., 2010; Ko et al., 2010); thus, *TET2* may regulate cell-fate decisions in adult stem/precursor cells as well. Indeed, RNAi-mediated depletion of *Tet2* in early hematopoietic precursors resulted in skewed differentiation, with an enhanced propensity to commit to the myeloid lineage in response to appropriate cytokines in vitro (Ko et al., 2010).

The gene expression changes observed in ESCs in response to acute *Tet1* depletion were consistent with the developmental effects observed in teratoma assays in vivo and embryoid body formation in vitro. Teratomas formed by Tet1 and Tet2-kd ESCs contained cells from all three germ layers, albeit with altered relative contributions compared to control ESCs, indicating that Tet1 and Tet2-kd ESCs retained pluripotency. Tet1-kd teratomas contained a high proportion of cells of the definitive endoderm and mesoderm lineages; cells of the neuroectoderm lineage were considerably fewer. Tet2-kd clones also formed large hemorrhagic teratomas but with greater contribution from neuroectoderm. These features are consistent with the role of Lefty proteins (positively regulated by Tet1, mildly repressed by Tet2) as inhibitors of the TGF-β family member Nodal. Downstream of Activin/Nodal receptors, moderate and strong inductive signals mediated by Smad2/3 support differentiation into mesoderm and definitive endoderm lineages marked by Brachyury and Foxa2 expression, respectively (Gadue et al., 2006; Kubo et al., 2004). Thus, diminished *Lefty* expression associated with *Tet1* depletion would be expected to increase Smad signaling under conditions where the Nodal pathway was active; increase expression of the downstream target of Nodal signaling, Eomes; increase Brachyury and Foxa2 expression in differentiation assays in vitro; and skew development toward mesoderm/endoderm lineages in vivo, exactly as actually observed. Reciprocally, the slight increase in *Lefty* expression caused by *Tet2* depletion would be expected to decrease Smad signaling and decrease the constraint on neuroectoderm gene expression. Although downregulation of *Pax6* upon *Tet1* depletion can also skew differentiation of mesendoderm by causing loss of neural progenitors, we did not observe any perceptible loss of Pax6 and NeuroD1 proteins when Tet1-depleted ESCs were differentiated for 4 days into embryoid bodies (data not shown). Thus, small changes in gene expression in Tet1-kd ESCs can be amplified into major changes in the strength of Nodal/Activin signaling, resulting in pronounced mesendoderm skewing during ESC differentiation.

Tet1-kd teratomas also showed a marked increase in the number of trophoblastic giant cells, especially amidst hemorrhagic and necrotic tissue. Furthermore, Tet1-kd ESCs chimerized placental tissue ectopically in midgestation stage embryos following blastocyst injection, albeit at low frequency. Again, this tendency was also apparent in vitro: Tet1-kd ESCs showed only a small increase in expression of the trophectoderm markers *Cdx2* and *Eomes* and did not express *Elf5*, but increased the expression of all three genes upon switching to TS culture conditions that promote derivation of trophoblast stem cells. Thus, an induction signal for differentiation (LIF withdrawal and supplementation with Fgf4 and heparin) accentuates the effect of *Tet1* deficiency on lineage commitment markers.

Our data suggest a complex relation between Tet proteins and DNA methylation. *Tet1* depletion resulted in increased DNA methylation at the *Lefty1* promoter in parallel with decreased expression of *Lefty1* mRNA and protein. These data are consistent with the possibility that Tet1 promotes hydroxymethylation of the *Lefty1* promoter, facilitating demethylation and, hence, promoting *Lefty1* transcription. This hypothesis is clearly inadequate in the case of *Elf5*, however. The *Elf5* promoter is normally silenced in ESCs by DNA methylation, and its demethylation and activation are required for ESCs to differentiate into trophoblast derivatives (Ng et al., 2008). In contrast, we find that *Tet1* depletion correlated with increased *Elf5* expression and trophectoderm skewing even though ESCs, ESCs cultured under TS conditions, and Tet1-kd ESCs cultured under TS conditions show similar hypermethylation at the *Elf5* promoter, compared to the hypomethylation observed in TS cells. Since conventional bisulfite sequencing does not distinguish 5mC and 5hmC (Huang et al., 2010; Jin et al., 2010; Nestor et al., 2010), we have not formally ruled out the possibility that 5hmC is present at a subset of CpG sites at the *Elf5* promoter. Although further studies are required to ascertain whether Tet1 binds directly to *Lefty*, *Elf5*, or other target genes, it is clear that the effect of Tet1 on DNA methylation and gene expression in ESCs cannot be explained by the simple postulate that 5hmC is an intermediate in a DNA demethylation pathway. Because Elf5 is located downstream of the trophoblast differentiation cascade and is induced by the early trophoblast lineage determinants Cdx2 and Eomes, one possibility is that *Tet1* depletion increases *Elf5* expression indirectly, through upregulation of *Cdx2* and *Eomes*.

In summary, our studies identify Tet proteins as key regulators of early embryonic differentiation. Our data suggest that these enzymes do not act alone but, rather, operate in coordination with developmental signals to regulate lineage determination at decision points that are critical for early lineage commitment. We propose that Tet1 functions downstream of Oct4 in the first lineage split between inner cell mass and trophectoderm to constrain *Elf5* expression in the inner cell mass; later in development, when the epiblast differentiates into the three somatic germ layers, Tet1 coordinates the canalization of developmental pathways by regulating *Lefty* (Figure S5). An understanding of the roles of Tet proteins and the epigenetic mark, 5hmC, in ESC function and embryonic development will require analysis of *Tet*-disrupted mice and the genome-wide localization of 5hmC.

EXPERIMENTAL PROCEDURES

Oct4 Binding Site Bioinformatics and Chromatin Immunoprecipitation

Alignments between the mouse and human Tet1 gene loci were performed on the Vista Browser (http://pipeline.lbl.gov/cgi-bin/gateway2) to include all intervening untranscribed regions between neighboring genes. Putative Oct4-Sox2 consensus sites were detected by the EMBOSS program

(http://emboss.sourceforge.net/docs/adminguide/node6.html) using the fuzznuc command line to detect the pattern "C[AT]TTGTN(0,5)ATGCAAAT" tolerating a mismatch of two bases. Predicted sites within CNS regions were manually assessed. PCR primers were designed to probe CNS regions at 1 kb intervals and are shown in Supplementary Information. ChIP reactions were performed as previously described (Rao et al., 2010). Samples were analyzed under similar conditions, and fold enrichments were calculated by comparing ChIP samples to genomic DNA controls after normalizing to GAPDH.

Teratoma Formation

Tumors and teratomas were obtained by intramuscular injection of 1×10^6 ESCs into each quadripcep of either NOD/SCID (Charles River Laboratories, Wilmington, MA) or $Rag2^{-/-};\gamma C^{-/-}$ mice with similar results. Specimens were collected when tumors exceeded 2.0 cm in diameter and were fixed overnight in 4% paraformaldehyde. Paraffin sections and staining were performed by the Specialized Rodent Histopathology Services at Brigham and Women's Hospital. Animal handling and maintenance were performed in accordance with institutional guidelines.

Chimera Generation

Fifteen ES or ES-TS cells labeled with GFP by lentiviral vectors were injected into mouse blastocysts and implanted by uterus transfer into pseudopregnant foster mothers using standard methods. Pregnant mice were sacrificed at day E10.5, and whole embryos were photographed with an inverted fluorescent microscope. Specimens were fixed overnight in 10% formalin, mounted in HistoGel (Richard-Allan Scientific, MI), and stored in 80% ethanol. Paraffin sections and anti-GFP staining were performed at the Specialized Rodent Histopathology Services, Brigham and Women's Hospital.

ESC Serum-free Embryoid Body Differentiation

CD4-Foxa2/GFP-Bry ESCs were maintained in serum-containing media with feeder cells before adaptation on feeder-free gelatin-coated wells in serum-free culture media (Invitrogen, Carlsbad, CA unless otherwise indicated) consisting of Knockout DMEM/F12 supplemented with 0.5× of both N2 and B27, penicillin/streptomycin, 0.05% BSA, LIF (1% conditioned medium), human BMP4 (10 ng/ml; R&D Systems, Minneapolis, MN), and 1.5×10^{-4} M 1-thioglycerol (Sigma, St. Louis, MO) as previously described (Gadue et al., 2006). ESCs were adapted for two passages in serum/feeder-free culture and transfected at 1.5×10^5 cells/ml for 2 days with 50 nM siRNA using Lipofectamine RNAiMAX according to manufacturer's instructions. To induce embryoid body (EB) differentiation (day 0), cells were dissociated by TrypLE Express and cultured at 1×10^5 cells/ ml in serum-free differentiation media consisting of 75% Iscove's modified Dulbecco's medium and 25% Ham's F12 media supplemented with 0.5× of both N2 and B27 (without retinoic acid), 0.05% BSA, 50 μg/ml ascorbic acid (Sigma), and 4.5×10^{-4} M 1-thioglycerol. At day 2, the EBs were dissociated with TrypLE Express and reaggregated in serum-free differentiation media with the addition of human activin A (R & D systems). Retransfections of siRNA were performed at days 0 and 2 of EB aggregation. At day 4, EBs generated were dissociated by incubation with trypsin and stained with anti-human CD4-phycoerythrin (BioLegend, San Diego, CA). The cells were analyzed by a FacsCalibur flow cytometer (Becton Dickinson, Franklin Lakes, NJ) and data processed with FlowJo software (TreeS Star, Ashland, OR). Note that Tet1 siRNA#1 and #2 correspond to Tet1 siRNA 1.1 and 1.2, respectively, in Figure S1A. For unknown reasons, Tet1 siRNA#1 was less effective than siRNA#2 in CD4-Foxa2/GFP-Bry ESCs, although in v6.5 ESCs, the two siRNAs were equivalent (see Figure S1A).

ACCESSION NUMBERS

Microarray data have been deposited in the GEO Database under the accession number GSE26900.

SUPPLEMENTAL INFORMATION

Supplemental Information includes five figures, one table, and Supplemental Experimental Procedures and can be found with this article online at doi:10.1016/j.stem.2011.01.008.

ACKNOWLEDGMENTS

We thank P. Gadue and G. Keller for CD4-Foxa2/GFP-Bry ESCs, C. Unitt and staff at the Specialized Rodent Histopathology Services, Brigham and Women's Hospital for mouse histology and GFP staining, P. Junni at the Finnish Microarray and Sequencing Centre, Turku Centre for Biotechnology for sample processing and array hybridization, and K. E. Waraska at the Biopolymers facility, Harvard Medical School, for low-density array-based q-PCR. This work was funded by NIH grants AI44432, CA42471, and RC1-DA028422 (to A.R.); RO1-DK70055, RO1-DK59279, UO1-HL100001, and special funds from the ARRA stimulus package RC2-HL102815 (to G.Q.D); the Roche Foundation for Anemia Research, Alex's Lemonade Stand, and the Harvard Stem Cell Institute (to G.Q.D); an American Heart Association postdoctoral fellowship (to K.P.K); and grants from The Academy of Finland and The Sigrid Juselius Foundation (to R.L.). G.Q.D. is an affiliate member of the Broad Institute, a recipient of Clinical Scientist Awards in Translational Research from the Burroughs Wellcome Fund and the Leukemia and Lymphoma Society, and an investigator of the Howard Hughes Medical Institute and the Manton Center for Orphan Disease Research. G.Q.D. is a member of the scientific advisory boards and holds stock in or receives consulting fees from the following companies: Johnson & Johnson, Verastem, Epizyme, iPierian, Solasia KK, and MPM Capital, L.L.P.

Received: June 22, 2010
Revised: December 16, 2010
Accepted: January 20, 2011
Published: February 3, 2011

REFERENCES

Arnold, S.J., Hofmann, U.K., Bikoff, E.K., and Robertson, E.J. (2008). Pivotal roles for eomesodermin during axis formation, epithelium-to-mesenchyme transition and endoderm specification in the mouse. Development *135*, 501–511.

Beddington, R.S., and Robertson, E.J. (1989). A. assessment of the developmental potential of embryonic stem cells in the midgestation mouse embryo. Development *105*, 733–737.

Besser, D. (2004). Expression of nodal, lefty-a, and lefty-B in undifferentiated human embryonic stem cells requires activation of Smad2/3. J. Biol. Chem. *279*, 45076–45084.

Boyer, L.A., Lee, T.I., Cole, M.F., Johnstone, S.E., Levine, S.S., Zucker, J.P., Guenther, M.G., Kumar, R.M., Murray, H.L., Jenner, R.G., et al. (2005). Core transcriptional regulatory circuitry in human embryonic stem cells. Cell *122*, 947–956.

Brennan, J., Lu, C.C., Norris, D.P., Rodriguez, T.A., Beddington, R.S.P., and Robertson, E.J. (2001). Nodal signalling in the epiblast patterns the early mouse embryo. Nature *411*, 965–969.

Chen, C., and Shen, M.M. (2004). Two modes by which Lefty proteins inhibit nodal signaling. Curr. Biol. *14*, 618–624.

Chen, X., Xu, H., Yuan, P., Fang, F., Huss, M., Vega, V.B., Wong, E., Orlov, Y.L., Zhang, W., Jiang, J., et al. (2008). Integration of external signaling pathways with the core transcriptional network in embryonic stem cells. Cell *133*, 1106–1117.

Chew, J.L., Loh, Y.H., Zhang, W., Chen, X., Tam, W.L., Yeap, L.S., Li, P., Ang, Y.S., Lim, B., Robson, P., et al. (2005). Reciprocal transcriptional regulation of Pou5f1 and Sox2 via the Oct4/Sox2 complex in embryonic stem cells. Mol. Cell. Biol. *25*, 6031–6046.

Delhommeau, F., Dupont, S., Della Valle, V., James, C., Trannoy, S., Masse, A., Kosmider, O., Le Couedic, J.P., Robert, F., Alberdi, A., et al. (2009). Mutation in TET2 in myeloid cancers. N. Engl. J. Med. *360*, 2289–2301.

Farthing, C.R., Ficz, G., Ng, R.K., Chan, C.F., Andrews, S., Dean, W., Hemberger, M., and Reik, W. (2008). Global mapping of DNA methylation in mouse promoters reveals epigenetic reprogramming of pluripotency genes. PLoS Genet. *4*, e1000116.

Feng, S., Cokus, S.J., Zhang, X., Chen, P.Y., Bostick, M., Goll, M.G., Hetzel, J., Jain, J., Strauss, S.H., Halpern, M.E., et al. (2010a). Conservation and

divergence of methylation patterning in plants and animals. Proc. Natl. Acad. Sci. USA *107*, 8689–8694.

Feng, S., Jacobsen, S.E., and Reik, W. (2010b). Epigenetic reprogramming in plant and animal development. Science *330*, 622–627.

Gadue, P., Huber, T.L., Paddison, P.J., and Keller, G.M. (2006). Wnt and TGF-beta signaling are required for the induction of an in vitro model of primitive streak formation using embryonic stem cells. Proc. Natl. Acad. Sci. USA *103*, 16806–16811.

Gal-Yam, E.N., Saito, Y., Egger, G., and Jones, P.A. (2008). Cancer epigenetics: modifications, screening, and therapy. Annu. Rev. Med. *59*, 267–280.

Goll, M.G., and Bestor, T.H. (2005). Eukaryotic cytosine methyltransferases. Annu. Rev. Biochem. *74*, 481–514.

Huang, Y., Pastor, W.A., Shen, Y., Tahiliani, M., Liu, D.R., and Rao, A. (2010). The behaviour of 5-hydroxymethylcytosine in bisulfite sequencing. PLoS ONE *5*, e8888.

Ito, S., D'Alessio, A.C., Taranova, O.V., Hong, K., Sowers, L.C., and Zhang, Y. (2010). Role of Tet proteins in 5mC to 5hmC conversion, ES-cell self-renewal and inner cell mass specification. Nature *466*, 1129–1133.

Ivanova, N., Dobrin, R., Lu, R., Kotenko, I., Levorse, J., DeCoste, C., Schafer, X., Lun, Y., and Lemischka, I.R. (2006). Dissecting self-renewal in stem cells with RNA interference. Nature *442*, 533–538.

Iyer, L.M., Tahiliani, M., Rao, A., and Aravind, L. (2009). Prediction of novel families of enzymes involved in oxidative and other complex modifications of bases in nucleic acids. Cell Cycle *8*, 1698–1710.

Jackson, M., Krassowska, A., Gilbert, N., Chevassut, T., Forrester, L., Ansell, J., and Ramsahoye, B. (2004). Severe Global DNA Hypomethylation Blocks Differentiation and Induces Histone Hyperacetylation in Embryonic Stem Cells. Mol. Cell. Biol. *24*, 8862–8871.

Jin, S.G., Kadam, S., and Pfeifer, G.P. (2010). Examination of the specificity of DNA methylation profiling techniques towards 5-methylcytosine and 5-hydroxymethylcytosine. Nucleic Acids Res. *38*, e125.

Kim, J., Chu, J., Shen, X., Wang, J., and Orkin, S.H. (2008). A. extended transcriptional network for pluripotency of embryonic stem cells. Cell *132*, 1049–1061.

Klose, R.J., and Bird, A.P. (2006). Genomic DNA methylation: the mark and its mediators. Trends Biochem. Sci. *31*, 89–97.

Ko, M., Huang, Y., Jankowska, A.M., Pape, U.J., Tahiliani, M., Bandukwala, H.S., An, J., Lamperti, E.D., Koh, K.P., Ganetzky, R., et al. (2010). Impaired hydroxylation of 5-methylcytosine in myeloid cancers with mutant TET2. Nature *468*, 839–843.

Kriaucionis, S., and Heintz, N. (2009). The nuclear DNA base 5-hydroxymethylcytosine is present in Purkinje neurons and the brain. Science *324*, 929–930.

Kubo, A., Shinozaki, K., Shannon, J.M., Kouskoff, V., Kennedy, M., Woo, S., Fehling, H.J., and Keller, G. (2004). Development of definitive endoderm from embryonic stem cells in culture. Development *131*, 1651–1662.

Lister, R., Pelizzola, M., Dowen, R.H., Hawkins, R.D., Hon, G., Tonti-Filippini, J., Nery, J.R., Lee, L., Ye, Z., Ngo, Q.-M., et al. (2009). Human DNA methylomes at base resolution show widespread epigenomic differences. Nature *462*, 315–322.

Loh, Y.H., Wu, Q., Chew, J.L., Vega, V.B., Zhang, W., Chen, X., Bourque, G., George, J., Leong, B., Liu, J., et al. (2006). The Oct4 and Nanog transcription network regulates pluripotency in mouse embryonic stem cells. Nat. Genet. *38*, 431–440.

Meissner, A., Mikkelsen, T.S., Gu, H., Wernig, M., Hanna, J., Sivachenko, A., Zhang, X., Bernstein, B.E., Nusbaum, C., Jaffe, D.B., et al. (2008). Genome-scale DNA methylation maps of pluripotent and differentiated cells. Nature *454*, 766–770.

Nestor, C., Ruzov, A., Meehan, R., and Dunican, D. (2010). Enzymatic approaches and bisulfite sequencing cannot distinguish between 5-methylcytosine and 5-hydroxymethylcytosine in DNA. Biotechniques *48*, 317–319.

Ng, R.K., Dean, W., Dawson, C., Lucifero, D., Madeja, Z., Reik, W., and Hemberger, M. (2008). Epigenetic restriction of embryonic cell lineage fate by methylation of Elf5. Nat. Cell Biol. *10*, 1280–1290.

Ooi, S.K.T., O'Donnell, A.H., and Bestor, T.H. (2009). Mammalian cytosine methylation at a glance. J. Cell Sci. *122*, 2787–2791.

Ramsahoye, B.H., Biniszkiewicz, D., Lyko, F., Clark, V., Bird, A.P., and Jaenisch, R. (2000). Non-CpG methylation is prevalent in embryonic stem cells and may be mediated by DNA methyltransferase 3a. Proc. Natl. Acad. Sci. USA *97*, 5237–5242.

Rao, S., Shao, Z., Roumiantsev, S., McDonald, L.T., Yuan, G.C., and Orkin, S.H. (2010). Differential Roles of Sall4 Isoforms in Embryonic Stem Cell Pluripotency. Mol. Cell. Biol. *30*, 5364–5380.

Reik, W., Dean, W., and Walter, J. (2001). Epigenetic reprogramming in mammalian development. Science *293*, 1089–1093.

Saijoh, Y., Adachi, H., Sakuma, R., Yeo, C.Y., Yashiro, K., Watanabe, M., Hashiguchi, H., Mochida, K., Ohishi, S., Kawabata, M., et al. (2000). Left-right asymmetric expression of lefty2 and nodal is induced by a signaling pathway that includes the transcription factor FAST2. Mol. Cell *5*, 35–47.

Schier, A.F. (2009). Nodal morphogens. Cold Spring Harb. Perspect. Biol. *1*, a003459.

Shen, M.M. (2007). Nodal signaling: developmental roles and regulation. Development *134*, 1023–1034.

Szwagierczak, A., Bultmann, S., Schmidt, C.S., Spada, F., and Leonhardt, H. (2010). Sensitive enzymatic quantification of 5-hydroxymethylcytosine in genomic DNA. Nucleic Acids Res. *38*, e181.

Tabibzadeh, S., and Hemmati-Brivanlou, A. (2006). Lefty at the crossroads of "stemness" and differentiative events. Stem Cells *24*, 1998–2006.

Tahiliani, M., Koh, K.P., Shen, Y., Pastor, W.A., Bandukwala, H., Brudno, Y., Agarwal, S., Iyer, L.M., Liu, D.R., Aravind, L., et al. (2009). Conversion of 5-methylcytosine to 5-hydroxymethylcytosine in mammalian DNA by MLL partner TET1. Science *324*, 930–935.

Takahashi, K., and Yamanaka, S. (2006). Induction of pluripotent stem cells from mouse embryonic and adult fibroblast cultures by defined factors. Cell *126*, 663–676.

Tam, P.P., and Loebel, D.A. (2007). Gene function in mouse embryogenesis: get set for gastrulation. Nat. Rev. Genet. *8*, 368–381.

Tanaka, S., Kunath, T., Hadjantonakis, A.K., Nagy, A., and Rossant, J. (1998). Promotion of trophoblast stem cell proliferation by FGF4. Science *282*, 2072–2075.

Yeom, Y.I., Fuhrmann, G., Ovitt, C.E., Brehm, A., Ohbo, K., Gross, M., Hubner, K., and Scholer, H.R. (1996). Germline regulatory element of Oct-4 specific for the totipotent cycle of embryonal cells. Development *122*, 881–894.

Ying, Q.-L., Nichols, J., Chambers, I., and Smith, A. (2003a). BMP Induction of Id Proteins Suppresses Differentiation and Sustains Embryonic Stem Cell Self-Renewal in Collaboration with STAT3. Cell *115*, 281–292.

Ying, Q.-L., Stavridis, M., Griffiths, D., Li, M., and Smith, A. (2003b). Conversion of embryonic stem cells into neuroectodermal precursors in adherent monoculture. Nat. Biotechnol. *21*, 183–186.

Zemach, A., McDaniel, I.E., Silva, P., and Zilberman, D. (2010). Genome-wide evolutionary analysis of eukaryotic DNA methylation. Science *328*, 916–919.